# Analyst

Accepted Manuscript






ROYAL SOCIETY OF CHEMISTRY

www.rsc.org/analyst

Journal Name

RSC Publishing

ARTICLE

# Synthesis of Fluorescent Dye-doped Silica Nanoparticles for Target-Cell-Specific Delivery and Intracellular MicroRNA Imaging

Cite this: DOI: 10.1039/x0xx00000x

Received ooth January 2012,
Accepted ooth January 2012

DOI: 10.1039/x0xx00000x

www.rsc.org/

Henan Li,‡[a] Yawen Mu,‡[b] Shanshan Qian,‡[a] Jusheng Lu,[a] Yakun Wan,[b] Guodong Fu,[a] and Songqin Liu[a*]

MicroRNA (miRNA) is found to be up-regulated in many kinds of cancer and therefore is classified as an oncomiR. Herein, we design a multifunctional fluorescent nanoprobe (FSiNPs-AS/MB) with AS1411 aptamer and molecular beacon (MB) co-immobilized on the surface of the fluorescent dye-doped silica nanoparticles (FSiNPs) for target-cell-specific delivery and intracellular miRNA imaging, respectively. The FSiNPs were prepared by a facile reverse microemulsion method from tetraethoxysilane and silane derivatized coumarin that was previously synthesized by click chemistry. The as-prepared FSiNPs possess uniform size distribution, good optical stability and biocompatibility. In addition, there is remarkable affinity interaction between AS1411 aptamer and nucleolin protein on cancer cell surface. Thus, a target-cell-specific delivery system by the FSiNPs-AS/MB is proposed for effectively transferring MB into the cancer cells to recognize the target miRNA. Using miRNA-21 in MCF-7 cells (a human breast cancer cell line) as model, the proposed multifunctional nanosystems not only allow target-cell-specific delivery with the binding affinity of AS1411, but also can track the simultaneously the transfected cells and detect intracellular miRNA in situ. The proposed multifunctional nanosystems are a promising platform for highly sensitive luminescent nonviral vector in biomedical and clinical research.

## Introduction

MicroRNAs (miRNAs) are a class of endogenous, small, non-coding regulatory RNAs (approximately 18-25 nucleotides) that regulate a wide array of biological processes such as cell proliferation, differentiation, and apoptosis.[1-4] Currently, the conventional miRNAs detection techniques include Northern blot, microarray and real-time polymerase chain reaction (RT-PCR).[5-7] Some of these methods have enabled label-free or even high-throughput detection of target miRNAs, and have been successfully implemented in clinical diagnostic procedures. However, these techniques require fixation or lysis of cells, miRNA isolation and/or target amplification, and thus cannot fully and repeatedly evaluate phenotypic diversity and cell-to-cell variations in miRNA expression.[8-11] Therefore, the development of efficient methods for rapid, specific, and sensitive detection of intracellular miRNAs is eagerly required.

Due to its unique thermodynamics and relatively low background, molecular beacons (MBs) detection of intracellular targets has attracted profound interest.[12, 13] Furthermore, MBs can offer a rapid method for monitoring intracellular miRNAs, because they do not require the separation of probe-target hybrids from excess non-hybridized probe or the isolation and amplification of RNA.[11, 14-16] For example, Kang et al.[16] have developed an MB composed of stem loop-structured DNA complementary to miRNAs, which successfully images miR-206 and miR-26a biogenesis during myogenesis using commercial transfection reagent. This system allows potential multiplex imaging of miRNAs, since several dye-quencher pairs can be applied simultaneously to a single cell. Dong et al.[14] have proposed an effective gene vector of polyethylenimine (PEI)-grafted graphene nanoribbon to deliver locked nucleic acid (LNA)-integrated MB to detect intracellular miRNA. However, many of these delivery systems can neither avoid nonspecific delivery nor be used to track the transfected cells.[17] Recently, many pioneered efforts have developed intracellular tracking systems based on nanostructured materials.[18-20] Well-tailored fluorescent dye-doped silica nanoparticles (FSiNPs) are highly attractive materials for delivery systems due to their unique versatility of fabrication techniques and functionality, which protects MB from degradation by endogenous nucleases and targets MB to specific cells.[21-23] The functional moiety on nanoparticles allows the conjugation of target-specific moieties, such as antibodies,[24] peptide,[23] aptamer,[25] and other molecules[20] that can recognize receptors on the cell surface. These multifunctional nanosystem can offer efficient delivery of MBs to target cell with fewer side effects, as well as the possibility to track transfected cells, thanks to the advanced optical properties of the nanosystem.[20, 23]

Generally, fluorescent dye molecules are introduced into silica nanoparticles by amino-terminated alkyltrialkoxysilane compounds such as (3-aminopropyl)triethoxysilane (APTS) and dye molecules with an isothiocyanate functional group.[26] However, an excess of amino-terminated alkyltrialkoxysilane has been used to co-condense

to form silica nanoparticles that allow an amount of amino terminal groups on the nanoparticles surface.[26] Previous studies have proved that such an excessive amount of amino-terminated alkyltrialkoxysilane produces adverse effect on the size uniformity.[27] More importantly, the amine groups on the surface make the obtained silica nanoparticles extremely difficult to stabilize in physiological conditions (i.e., aqueous solution, pH 7-7.5), where most biological experiments are carried out, and lead to a high cytotoxicity.[28, 29] As one option to address these challenges, therefore, the development of a new synthetic method to prepare FSiNPs without employing amino-terminated alkyltrialkoxysilane for the thiourea linkage formations is highly anticipated.

Herein, we design a multifunctional FSiNPs nanoprobe, which contains a cell-targeting moiety, as well as a conjugated MB to specifically recognize the target miRNA sequence. The FSiNPs were synthesized by a facile reverse microemulsion method from tetraethoxysilane (TEOS) and silane derivatized fluorescent organic dye molecules, which were successfully synthesized by click chemistry without employing amino-terminated alkyltrialkoxysilane compounds for the thiourea linkage formations (Scheme 1). The aptamer, named AS1411, has extensively proved capable of specifically binding nucleolin on cell surface and has already been used as a cancer-targeting delivery vehicle for several types of nanoparticles.[30, 31] Combining the remarkable affinity and specificity of AS1411 aptamer to target cancer cells, the MB could be unloaded only inside targeted cancer cells to detect target miRNA; the disulfide linkages between MB and the nanoparticles should be cleaved in the intracellular reductive environment in the presence of glutathione.[23] Using miRNA-21 in MCF-7 cells (a human breast cancer cell line) as a model, a method for simultaneous tracking of the transfected cells and in situ detection of intracellular miRNA by the multifunctional FSiNPs nanoprobe is reported.

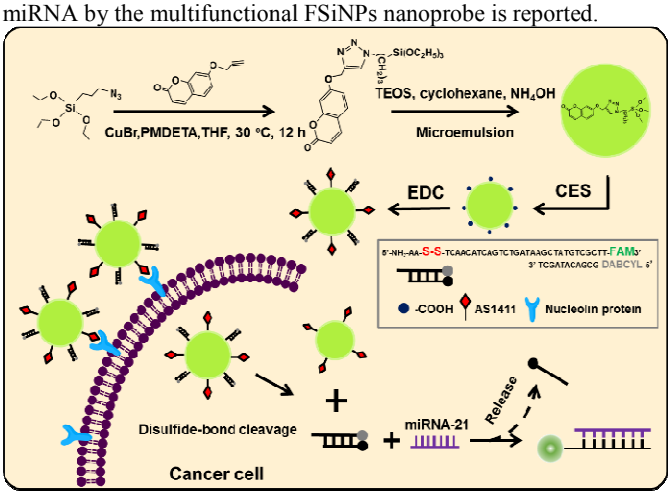


**Scheme 1.** Schematic of the synthesis of FSiNPs, and multifunctional nanoprobes for target specific imaging and intracellular detection of miRNA.

## Experimental

### Materials and reagents

Tetraethoxysilane (TEOS), 3-chloropropyltriethoxysilane, formaldehyde, 1-ethyl-3-(3- dimethylaminopropyl) carbodiimide hydrochloride (EDC) and pentamethyldiethylenetriamine (PMDETA) were from Sigma-Aldrich Inc. (USA). Propargyl bromide and 7-hydroxy coumarin were purchased from J&K Chemical Ltd. (Shanghai). Copper (I) bromide (CuBr) and sodium azide were obtained from Shanghai Chemical Reagent Plant (Shanghai, China). Triton X-100 was from Acros Organic Co. of Geel (Belgium). Carboxyethylsilanetriol sodium salt (CES, 25% in water) was from Gelest Inc. (USA). 3-(4,5-Dimethylthiazol-2-yl)-2-diphenyltetrazolium bromide (MTT), Annexin V-FITC and propidium iodide (PI) were purchased from KeyGen Biotech. Co. Ltd. (Nanjing, China). All other reagents were of analytical grade.

The oligonucleotides were purchased from Sangon Biological Engineering Technology & Co. Ltd. (Shanghai, China). The molecular beacon (MB) for miRNA-21 in MCF-7 cancer cells was designed by an intact complementary DNA with fluorescent dye of FAM at 3'-end and -$NH_2$-AA-S-S- at 5'-end that were used for coupling with FSiNPs. The MB hybridized with a short oligonucleotide composing of DABCYL at 5'-end, which allowed it to quench the fluorescence of FAM. Their sequences were:
AS1411 apatmer:
5'-$NH_2$-TTGGTGGTGGTGGTTGTGGTGGTGGTGG-3';
The long ligonucleotide ($MB_L$) containing the miRNA-21 binding sequence, which is a perfectly reverse complimentary sequence against mature miRNA-21:
5'-$NH_2$-AA-S-S-TCAACATCAGTCTGATAAGCTATGTCGCTT-FAM-3';
Short oligonucleotide: 5'- DABCYL-GCGACATAGCT-3'.

### Apparatus and characterization

$^1$H spectra were recorded on AVANCE II 400 MHz spectrometer (Bruker, Germany) with tetramethylsilane as internal standard. The Fourier transform infrared (FT-IR) spectra of the samples were obtained with Nicolet Nexus 470 FT-IR Spectrometer (Thermo Nicolet, USA). The morphologies of the FSiNPs were investigated by using transmission electron microscopy (TEM, JOEL JEM-2010, Japan). Fluorescence spectra were recorded on FluoroMax-4 spectrofluorometer with Xenon discharge lamp excitation (HORIBA, USA). Zeta potentials and particles sizes of the FSiNPs were determined at room temperature by a Zeta Plus Potential Analyzer (Brookhaven Instruments Corporation, USA). The electrochemical experiments were performed with a CHI750 C electrochemical analyzer (Chen Hua Instruments, Shanghai, China) with a conventional three-electrode system where glassy carbon electrode (GCE, 3 mm in diameter) was used as working electrode, a saturated calomel electrode (SCE) as reference electrode and platinum wire as counter electrode, respectively.

### Synthesis of 3-azidopropyltriethoxysilane

3-Chloropropyltriethoxysilance (41.7 mmol), sodium azide (77mmol), and dry DMF (50 mL) were added to a two-necked round-bottomed flask. The solution was heated to 90 ºC under a nitrogen atmosphere for 5 h. The low-boiling compounds were removed by distillation under reduced pressure, crystallization in 100 mL dry THF, filtration and removing the solvent under vacuum. Finally, distillation of the residual oil under reduced pressure at 40 ºC gave the desired product as colorless liquid.

### Synthesis of 7-propinyloxy coumarin

7-propinyloxy coumarin was prepared according to Chen's work.[32] 7-Hydroxy coumarin (20 mmol), $K_2CO_3$ (20 mmol), KI (1 mmol), propargyl bromide (25 mmol) and acetone (50 mL) were added to a flask, and the solution was stirred overnight at 80 ºC. Then the reaction mixture was cooled to room temperature and extracted with $CH_2Cl_2$ (3 × 50 mL). The combined organic extracts were washed with water (2 × 50 mL), dried over anhydrous $MgSO_4$ and evaporated to afford a crude product, which was purified by recrystallization from anhydrous ethanol to give a white solid.

### Preparation of FSiNPs

Cycloadditon reactions of 3-azidopropyltriethoxysilane with 7-propinyloxy coumarin were carried out under nitrogen using Schlenk tubes. Typical experimental procedures are given below. 3-azidopropyltriethoxysilane (0.243 mmol), 7-propinyloxy coumarin (0.243 mmol), PMDETA (0.12 mmol) and CuBr (0.12mmol) were placed in a 15 mL Schlenk tube. THF (2 mL) was then injected into the solution. After stirring at 30 ºC for 12 h, the reaction mixture was diluted with THF (3 mL) and passed through a column of neutral alumina. The supernatant was decanted and concentrated.

Briefly, Triton X-100 (1.77 mL), cyclohexane (7.5 mL), 1-hexanol (1.8 mL) and ultrapure water (340 µL) was mixed together with continuous stirring. Then, TEOS (100 µL) and coumarin-functionalized siloxane (25 µL) was added. The polymerization reaction was initiated by adding $NH_3 \cdot H_2O$ (60 µL, 28%). The reaction was allowed to stir for 24 h at 4 ºC. The reaction was terminated by adding ethanol. The FSiNPs were collected by centrifugation, washing with ethanol and water, drying in a vacuum at room temperature.

### Covalent conjugation of AS1411 or/and MB to FSiNPs

Carboxyl group derivatization was accomplished according to Wang's work.[33] Typically, 10 mg of FSiNPs and 20 µL of CES were added to 10 mM pH 7.4 phosphate buffer (PB) (1 mL) and were kept stirred for 3 h. The resultant FSiNPs functionalized with carboxyl group (FSiNPs-COOH) were then washed with PB for three times and re-dispersed in the same buffer to a final volume of 2 mL. Then, 5 nM of AS1411, or 5 nM of miRNA-21 MB, or a mixture of 5 nM AS1411 and 5 nM miRNA-21 MB were added to 2 mg $mL^{-1}$ FSiNPs-COOH in the presence of 0.5 µM EDC, respectively. The reaction was allowed to progress at room temperature for 1 h. For the miRNA-21 MB conjugated FSiNPs, 5 nM short oligonucleotide tagged with Dabcyl quencher was further added to hybridize with MB and quench the fluorescent FAM in MB for another 1 h. After centrifugation and washing, the AS1411 or/and miRNA-21 MB conjugated FSiNPs (FSiNPs-AS, FSiNPs-MB and FSiNPs-AS/MB, respectively) were obtained and stored at 4 ºC for later use.

### Cytotoxicity assay and apoptosis experiment

For cytotoxicity assay, MCF-7 cells (~ $5.0 \times 10^3$) were cultivated in 100 µL media in each well of a 96-well plate for 12 h. After discarding the media, fresh medium alone or medium containing FSiNPs was added to each well of the 96-well plate and cultivated for another 24 h. 20 µL MTT (5 mg $mL^{-1}$) was then added to each well. After incubation for 4 h, the medium was removed and 150 µL sodium dodecyl sulfate was added to each well to solubilize the formazan dye. After vortexing for 15 min, the absorbance of each well was measured using a model 550 microplate reader Bio-Rad 550 at 570 nm (Bio-Rad, USA).

The apoptosis experiments were carried out with Annexin V-FITC/PI double staining. The cells (~ $4.0 \times 10^5$) were seeded for 12 h in a 6-well plate containing DMEM (2 mL) in each well. The culture medium was then replaced with fresh medium containing FSiNPs and cultured for another 24 h. The resulting cells were harvested, then stained with Annexin V-FITC/PI for 10 min in accordance to manufacturer's instruction. The MCF-7 cells were then collected and analyzed by flow cytometry on FACS Calibur flow cytometer (Becton Dickinson, USA).

### Confocal laser microscopy assay

Cancer and normal cells ($1 \times 10^4$ cell/one 24 well) were seeded on 25-mm-diameter glass cover slips and the cells were grown for 12 h at 37 ºC. After the cells were washed with phosphate buffered saline (PBS) for three time, 500 µL fresh DMEM containing 100 µg $mL^{-1}$ FSiNPs-AS or FSiNPs-AS/MB was dropped and incubated at 37 ºC for 3 h. The cells were fixed by gentle shaking for 20 min with 4% paraformaldehyde solution. The cells were then washed three times with PBS for 10 min, and cover-slipped with mounting medium. The cells were imaged by confocal laser scanning microscopy (Leica TCS SP5 II, Germany).

## Results and discussion

### Synthesis and characterization of FSiNPs

3-Azidopropyltriethoxysilane was synthesized by reaction of 3-chloropropyltriethoxysilane with sodium azide in dry dimethylformanide (DMF). After introduction of azide, a new absorption peak appeared at ~ 2100 $cm^{-1}$ in the FT-IR spectra (Figure S1), which corresponded to the vibration of the pendant azido groups in 3-azidopropyltriethoxysilane.[34] The $^1H$ NMR spectrum showed characteristic signals at around 1.21 (9H), 3.81 (6H), 3.34 (2H), 1.66-1.70 (2H), and 0.66 (2H) ppm, which corresponded to the protons of methyl and methylene, respectively (Figure S2). These results confirmed successful synthesis of 3-azidopropyltriethoxysilane.

A characteristic peak at ~ 3280 $cm^{-1}$ in the FT-IR spectra corresponded to alkyne groups (Figure S1). The $^1H$ NMR signals at around 7.62-7.68 (1H), 7.37-7.63 (1H), 6.88-6.97 (2H), and 6.24-6.32 (1H) ppm were attributed to the aromatic protons. The $^1H$ NMR signals at around 4.76-4.80 (2H) and 2.55-2.62 (1H) ppm corresponded to the protons of methylene and propargyl, respectively (Figure S3), which confirmed that propargyl group were introduced independently into hyroxyl functional coumarin.[35] Coumarin-functionalized siloxane was prepared by the cycloaddition reaction of 3-azidopropyltriethoxysilane and 7-propinyloxy coumarin. After the cycloaddition reaction, the peak of azide or alkyne disappeared from its FT-IR spectra (Figure S1), confirming the formation of triazole rings in coumarin-functionalized siloxane.

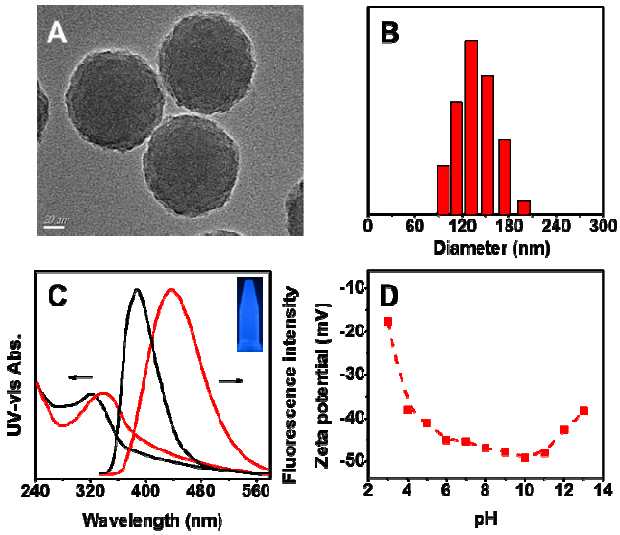


**Figure 1.** (A) TEM image of FSiNPs. (B) Particle size distributions of FSiNPs. (C) Absorbance and fluorescence emission spectra (λex = 320 nm) of 7-prpinyloxy coumarin (black) and FSiNPs (red) in ethanol. Inset: FSiNPs suspension under 365 nm irradiation. (D) Zeta potential of FSiNPs as a function of pH.

The FSiNPs were prepared via a reverse microemulsion method with coumarin-functionalized siloxane as precursor. The TEM image showed that the as-prepared FSiNPs had a nearly spherical shape and uniform size of ~ 90 nm (Figure 1A). Particle size distribution measurement showed that the mean diameter of FSiNPs was 135 nm larger than that from the TEM observation (Figure 1B). This would

be due to the surface charge of FSiNPs that created an electrical double layer and resulted in an increased colloidal hydrodynamic radius.[36] The FSiNPs displayed a strong absorption peak at ca. 339 nm, which corresponded to coumarin moiety (Figure 1C).[32] It emitted

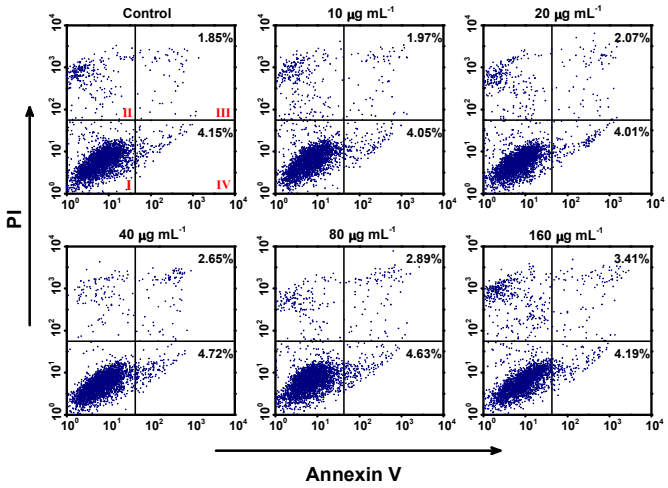


**Figure 2.** Flow cytometry analysis of apoptosis in MCF-7 cells treated with various concentrations of FSiNPs.

bright blue luminescence when excited by 365 nm ultraviolet lamp, and had a PL quantum yield of ~ 16% (Inset in Figure 1C). The PL spectrum of FSiNPs showed the strongest peak at 440 nm with an excitation wavelength of 320 nm. The UV and PL spectrum of FSiNPs were broadened and shifted to red by about 20 nm and 40 nm, respectively, compared to that of 7-propinyloxy coumarin. The enhanced fluorescence intensity of coumarin chromophore may have been due to the formation of π~π stacked aggregation when dye was embedded into the silica nanoparticles,[37] and/or the electron-donating property of the 1,2,3-triazole ring.[38]

The fluorescence pH dependence and the photostability of FSiNPs were investigated. The fluorescence of FSiNPs remained constant from pH 4 to 13, and changed less than 8 % at pH 3 after 30 min incubation (normalized by fluorescence at pH 7). The high photostability of FSiNPs may have resulted from the restricted movement of dye molecules after being chemically bound to the silica matrix, which provided resistance to photo-bleaching.[27, 39] In addition, the high surface charge of FSiNPs contributed to colloidal stability due to strong electrostatic repulsion between the nanoparticles. The high surface charge of FSiNPs was supported by zeta potential measurement (Figure 1D). The zeta potentials of FSiNPs in pH range from 3 to 10 were negatively signed. Several commonly used physiological buffers were chosen to test photostability through measurements of the temporal fluorescence of the FSiNPs. The results suggested that the FSiNPs were very stable in PBS, DMEM and Roswell Park Memorial Institute 1640 (RPMI 1640) during the initial 42 h of incubation (Figure S4). This result was quite different from the dye-doped silica nanoparticles prepared from amino-terminated alkyltrialkoxysilane and dye molecules directly, which possess lower stability and dispersion in ethanol and water at pH ≥ 7.[36]

## Cytotoxicity

The cytotoxicity of FSiNPs was evaluated by 3-(4,5-dimethylthiazol-2-yl)- 2,5-diphenyltetrazolium bromide (MTT) assay. MCF-7 cells served as models cultivated in media containing FSiNPs with various dosages of 10, 20, 40, 80 and 160 μg $mL^{-1}$ for 24 h. The cell viability are maintained at 97, 96, 93, 93 and 91% respectively in each case, which indicated low cytotoxicity of the as-prepared FSiNPs (Figure S5). The lower cytotoxicity of the FSiNPs may have resulted from its negatively charged surface, which lowered affinity to the negatively charged cell membrane, and decreased necrosis of the cells.[40] Figure 2 showed the flow cytometry graphs of the cells with various dosages of the FSiNPs. Annexin V-FITC emission signal is plotted on the x-axis, and PI emission signal is plotted on the y-axis. Control group was incubated in the absence of FSiNPs and displayed an apoptotic ratio of 6.0%. After incubation with 10, 20, 40, 80 and 160 μg $mL^{-1}$ of FSiNPs, the corresponding ratio of apoptosis are 6.0, 6.1, 7.4, 7.5, and 7.6%, respectively, which was consistent with the above results and indicates that the FSiNPs induced little cytotoxicity for the cells.

## Construction of multifunctional nanoprobes

The multifunctional nanoprobes were constructed by co-immobilization of AS1411 and miRNA-21 MB on FSiNPs using aqueous carbodiimide coupling chemistry. Following this coupling step, the short oligonucleotide tagged with Dabcyl quencher was further hybridized with MB to quench the fluorescent of FAM in MB. The preparation of FSiNPs-AS/MB was confirmed by zeta potential analysis and electrochemical impedance spectrum. The mean zeta potential for FSiNPs was negative (-45.3 mV). After functionalization with CES, the FSiNPs-COOH showed a much further negative zeta potential (-54.7 mV), which indicated successful functionalization of FSiNPs by the carboxyl group. After coupling with AS1411 and MB, the surface potential of FSiNPs-AS/MB changes further negative with zeta potential of -66.8 mV, which was attributed to the more negative phospholipids of AS1411 and MB linked to FSiNPs (Figure 3A). The electrochemical impedance spectrum revealed that the electron transfer resistance increased from 213 Ω for FSiNPs to 382 Ω for FSiNPs-COOH and 746 Ω for FSiNPs-AS/MB due to the increased electrostatic repulsion between $Fe(CN)_6^{3-/4-}$ redox probe and both negatively charged carboxyl and DNA strand (Figure 3B). These results confirmed that the FSiNPs successfully functionalized with both carboxyl and DNA.

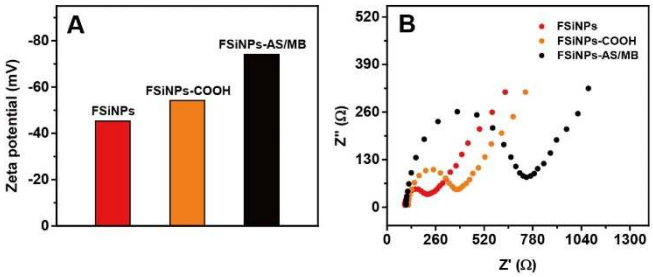


**Figure 3.** (A) Zeta potential of FSiNPs, FSiNPs-COOH, and FSiNPs-AS/MB. In these experiments, the FSiNPs were dispersed in ultrapure water. (B) EIS of FSiNPs, FSiNPs-COOH, and FSiNPs-AS/MB modified GCEs in 0.1 M KCl containing 5 mM $Fe(CN)_6^{3-/4-}$. Electrochemical impedance measurements (EIS) were obtained in a 0.1 M KCl solution containing 5 mM $Fe(CN)_6^{3-/4-}$ with a frequency range from 0.01 Hz to 100 kHz at 0.24 V. The amplitude of the applied sine wave potential in each case was 5 mV.

After functionalization with AS1411 and MB, the FSiNPs-AS/MB also emitted bright blue luminescence as FSiNPs itself, and negligible fluorescent of FAM at around 518 nm due to the fluorescent quenching by Dabcyl quencher (Figure 4A, curve a). Upon addition of target miRNA-21, the short DNA tagged with Dabcyl quencher that hybridized 11-base with MB was released from MB due to the intensive interaction between MB and miRNA-21. This allowed a sharp enhancement of the fluorescence intensity

of FAM (Figure 4A, curve b). Moreover, no effective fluorescence resonance energy between FAM and FSiNPs was observed due to the long distance between two chromophores (32 -mer oligonucleotide, appro. 10.88 nm based on the distance between DNA bases of 0.34 nm).[41, 42] The recovery of the fluorescence of FAM in the presence of target miRNA-21 permitted quantification of the miRNA-21 concentration by FSiNPs-AS/MB. The fluorescence intensity of FAM was found to be proportional to the concentration of miRNA-21 in the incubation solution, within a calibration range from 0.5 to 50 nM (Figure 5B). The linear curve was fitted by a regression equation of I = 1.17 × 106 + 66262.58 c (nM), in the linear range from 1 nM to 40 nM with a coefficient of determination of $R^2$ = 0.9888, where I is the fluorescence intensity and c is the miRNA-21 concentration (Inset in Figure 4B). The detection limit was 0.3 nM at signal-to-noise ratio of 3. The intraassay and interassay variation coefficients (CVs) obtained from 1 nM target miRNA-21 were 5.4% and 7.6%, which indicated an acceptable reproducibility and precision.

The sequence specificity of gene probe was studied. For comparison, miRNA-21 target with miRNA-16 target and miRNA-26a target were used under the same conditions. The response to miRNA-16 and miRNA-26a did not obviously change in comparison to the background fluorescence. The perfectly complementary miRNA-21 target showed a fluorescence intensity larger than that for miRNA-16 sequence and miRNA-26a sequence, respectively (Figure S6). The specificity of the proposed gene probe was also evaluated by measuring the fluorescent intensity of a mixed sample composed of miRNA-21, miRNA-16, and miRNA-26a. No significant change of intensity difference could be observed as compared to the result obtained in the presence of miRNA-21 only. These results suggested that the proposed gene probe was of high sequence specificity.

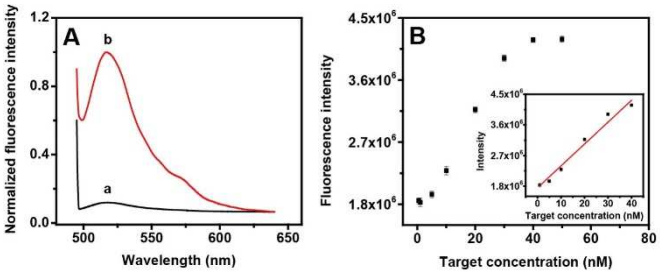


**Figure 4.** (A) Emission fluorescence spectra of FSiNPs-AS/MB in (a) absence and (b) presence of target DNA ($\lambda_{ex}$ = 480 nm). (B) Plot of the fluorescence intensity vs the concentration of target. Inset: linear plot for target determination.

**Target-cell-specific delivery and cancer cells imaging**

Target-cell-specific delivery is very important for the development of diagnosis, because it can limit side effects from nonspecific delivery and reduce the quantity of gene probe needed for treatment.[20] The AS1411 aptamer was linked to FSiNPs as a target-specific moiety. MCF-7 cell is well known for expressing nucleolin protein on its cell membrane. As shown in the confocal blue-field image in Figure 6, after incubation of FSiNPs-AS with MCF-7 cells at 37 ºC for 3 h, some fluorescent spots were clearly observed. In contrast, no obviously fluorescent spots could be observed after MCF-7 cells were treated with FSiNPs and FSiNPs-MB in the absence of AS1411, respectively (Figure S7 A, B), which indicated that the nonspecific interactions between nanoparticles and MCF-7 cells were negligible. Also, no fluorescence signal was observed using a nucleolin protein-negative human normal mammary epithelial cell line (MCF-10A) instead of MCF-7 cells, treated with FSiNPs-AS under the same conditions (Figure 5B). The selectivity of nanoprobes was tested with a cell mixture. Different ratios of MCF-7 (positive cell) to MCF-10A cells were co-cultures in a 12-well plate. After treated with Then 500 μL fresh DMEM containing 100 μg $mL^{-1}$ FSiNPs-AS was dropped and incubated at 37 ºC for 3 h. Then the harvested cells were studied using flow cytometric measurements. As the percentage of MCF-7 in the cell mixture increased from 0% to 100%, the percentage of positive signals obtained with the FSiNPs-AS increased accordingly, from 3.2% to 84.7%. A linear positive correlation was obtained between the percentage of MCF-7 cells input (x axis) and percentage of positive cells identified (y axis) with a correlation coefficient of 0.9622, indicating that the FSiNPs-AS can effectively target to tumor cells. (Figure S8). All these results demonstrated that the FSiNPs-AS retained the AS1411 binding activity. The FSiNPs-AS could be used for targeting tumor cells which possessed large numbers of nucleolin protein on the cell membrane. The attachment of FSiNPs to MCF-7 cells was due to the highly specific interaction between AS1411 aptamer linked to FSiNPs and nucleolin protein on the cell membrane.

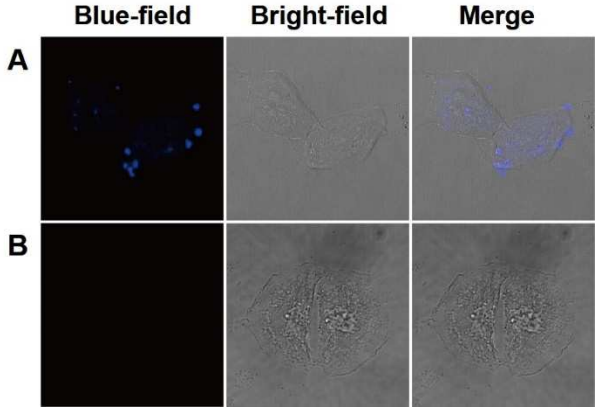


**Figure 5.** Confocal blue-field, bright-field and merge images of MCF-7 cells (A) and (B) MCF-10A cells treated with FSiNPs-AS (100 μg $mL^{-1}$) at 37 ºC for 3 h.

After incubation of FSiNPs-AS/MB nanoprobes with MCF-7 cells, two kinds of fluorescence spots with blue for FSiNPs and green for FAM were clearly observed in the cytoplasm of the MCF-7 cells at blue field and green field, respectively (Figure 6). The green fluorescence came from the recovery of the fluorescence of FAM in the presence of intracellular miRNA-21, which released the short DNA tagged with Dabcyl quencher from MB. The overlay image showed the separation of the blue and green fluorescence associated to FSiNPs and FAM, respectively, proved the MB was effectively released from the FSiNPs. The release of MB occurred through the cleavage of the disulfide linkage between the MB and FSiNPs in the intracellular reductive environment in the presence of glutathione.[20, 23] To confirm the cleavage of the disulfide linkage, an approach based on electrophoresis (see the Supporting Information).[43] The analysis showed that the disulfide linkage was indeed cleaved in reductive condition. The All these results revealed that FSiNPs-AS/MB nanoprobes delivered the MB into the cells. The recognition between intracellular miRNA-21 and MB produced green fluorescence of the dye due to the separation of the dye from the quenchers. The FSiNPs-AS/MB nanoprobes could be used not only for target-cell-specific delivery with binding affinity of AS1411, but also for imaging of the intracellular miRNA-21.

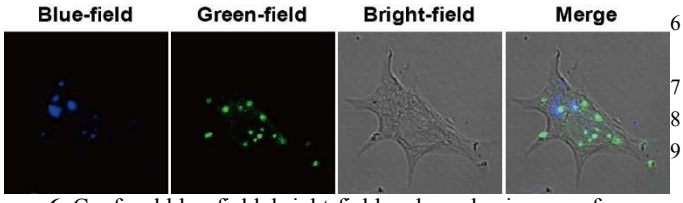


**Figure 6.** Confocal blue-field, bright-field and overlay images of MCF-7 cells treated with FSiNPs-AS/MB (100 μg $mL^{-1}$) at 37 ºC for 3 h.

## Conclusions

In summary, we develop a dual-functional nanoprobe for target-cell-specific delivery and intracellular miRNA imaging. The FSiNPs were prepared by a reverse micromulsion method with coumarin-functionalizaed siloxane precursor that was synthesized by cycloaddition reaction. The obtained FSiNPs exhibited excellent fluorescence stability, in pH range from 3 to 11, and superior photophysical stability under physiological conditions. The cell-specific targeting of nanoprobes by AS1411 conjugation has been verified. The recognition between intracellular miRNA-21 and MB produced green fluorescence of the dye due to the separation of the dye from the quenchers, which led the nanoprobes to be used not only for target-cell-specific delivery with the binding affinity of AS1411 but also for simultaneously tracking the transfected cells and detecting in situ intracellular miRNA-21. The proposed FSiNPs-AS/MB nanoprobes would be a promising platform for highly sensitive luminescent nonviral vector in biomedical and clinical research.

## Acknowledgements

This work was supported by National Basic Research Program of China (No. 2010CB732400), the Key Program (21035002) from the National Natural Science Foundation of China, National Natural Science Foundation of China (Grant Nos. 21375014), and the Fundamental Research Funds for the Central Universities.

## Notes and references

[a] *School of Chemistry and Chemical Engineering, Southeast University, Jiangning District, Nanjing, 211189, P.R. China.*Address here.
[b] *Institute of Life Sciences, Joint Center for Nanobody R&D between SEU and Egens Bio, Southeast University, Sipailou District, Nanjing, 210000, P.R. China.*Address here.
**Corresponding author at: School of Chemistry and Chemical Engineering, Southeast University,*
*E-mail: liusq@seu.edu.cn (S. Q. Liu)*
*‡ H. N. Li, Y. W. Mu and S. S. Qian contributed to this work equally.*
Electronic Supplementary Information (ESI) available: including details of FT-IR spectra, 1H NMR spectra, colloidal stability, cytotoxicity, and quantum yield. See DOI: 10.1039/b000000x/

1 V. Ambros, *Nature*, 2004, **431**, 350.
2 D. P. Bartel, *Cell*, 2004,**116**, 281.
3. P. D. Zamore and B. Haley, *Science*, 2005, **309**, 1519.
4 E. H. Noh, H. Y. Ko, H. Lee, M. S. Jeong, Y. W. Chang, and S. Kim, *J. Mater. Chem. B*, 2013, **1**, 4438.
5 M.S. Kumar, J. Lu, K.L. Mercer, T.R. Golub, and T. Jacks, *Nat. Genet.*, 2007, **39**, 673.
6 J. M. Thomson, J. Parker, C. M. Perou, and S. M. Hammond, *Nat. Methods*, 2004, **1**, 47.
7 É. Várallyay, J. Burgyán, and Z. Havelda, *Nat. Protoc.*, 2008, **3**, 190.
8 J. Q. Yin, R. C. Zhao, and K. V. Morris, *Trends Biotechnol.*, 2008, **26**, 70.
9 H. Dong, J. Lei, L. Ding, Y. Wen, H. Ju, and X. Zhang, *Chem. Rev.*, 2013, **113**, 6207.
10 C. Chen, D. A. Ridzon, A. J. Broomer, Z. Zhou, D. H. Lee, J. T. Nguyen, M. Barbisin, N. L. Xu, V. R. Mahuvakar, M. R. Andersen, K. Q. Lao, K. J. Livak, and K. J. Guegler, *Nucleic Acids Res.*, 2005, **33**, e179.
11 W. J. Kang, Y. L. Cho, J. R. Chae, J. D. Lee, B. A. Ali, A. A. Al-Khedhairy, C. H. Lee, and S. Kim, *Biomaterials*, 2012, **33**, 6430.
12 S. Tyagi, S. A. Marras, and F. R. Kramer, *Nat. Biotechnol.*, 2000, **18**, 1191.
13 K. Wang, Z. Tang, C. J. Yang, Y. Kim, X. Fang, W. Li, Y. Wu, C. D. Medley, Z. Cao, J. Li, P. Colon, H. Lin, and W. Tan, *Angew. Chem. Int. Ed.*, 2009, 48, 856.
14 H. Dong, L. Ding, F. Yan, H. Ji, and H. Ju, *Biomaterials*, 2011, **32**, 3875.
15 Z. Foldes-Papp, K. Konig, H. Studier, R. Buckle, H. G. Breunig, A. Uchugonova, and G.M. Kostner, *Curr. Pharm. Biotechnol.*, 2009, **10**, 569.
16 W. J. Kang, Y. L. Cho, J. R. Chae, J. D. Lee, K. J. Choi, and S. Kim, *Biomaterials*, 2011, **32**, 1915.
17 H. Dong, J. Lei, H. Ju, F. Zhi, H. Wang, W. Guo, Z. Zhu, and F. Yan, *Angew. Chem. Int. Ed.*, 2012, **51**, 4607.
18 D. S. Seferos, D. A. Giljohann, H. D. Hill, A. E. Prigodich, and C. A. Mirkin, *J. Am. Chem. Soc.*, 2007, **129**, 15477.
19 J. Conde, J. Rosa, J. M. de la Fuente, and P. V. Baptista, *Biomaterials*, 2013, **34**, 2516.
20 J. Conde, M. Larguinho, A. Cordeiro, L. R. Raposo, P. M. Costa, S. Santos, M. S. Diniz, A. R. Fernandes, P. V. Baptista, *Nanotoxicology*, 2014, **8**, 521.
21 K. Wang, X. He, X. Yang, and H. Shi, *Acc. Chem. Res.*, 2013, **46**, 1367.
22 J. E. Smith, C. D. Medley, Z. Tang, D. Shangguan, C. Lofton, and W. Tan, *Anal. Chem.*, 2007, **79**, 3075.
23 J. H. Lee, K. Lee, S. H .Moon, Y. Lee, T. G. Park, and J. Cheon, *Angew. Chem. Int. Ed.*, 2009, **48**, 4174.
24 E. Song, P. Zhu, S. K. Lee, D. Chowdhury, S. Kussman, D. M. Dykxhoorn, Y. Feng, D. Palliser, D. B. Weiner, P. Shankar, W. A. Marasco, and J. Lieberman, *Nat. Biotechnol.*, 2005, **23**, 709.
25 J. O. McNamara, E. R. Andrechek, Y. Wang, K. D. Viles, R. E. Rempel, E. Gilboa, B. A. Sullenger, and P. H. Giangrande, *Nat. Biotechnol.*, 2006, **24**, 1005.
26 S. W. Ha, C. E. Camalier, G. R. Beck Jr., and J. K. Lee, *Chem. Common.*, 2009, 2881.
27 M. Nakamura, M. Shono, and K. Ishimura, *Anal. Chem.*, 2007, **79**, 6507.
28 C. Earhart, N. R. Jana, N. Erathodiyil, and J. Y. Ying, *Langmuir*, 2008, **24**, 6215.
29 A. Nan, X. Bai, S. J. Son, S. B. Lee, and H. Ghandehari, *Nano Lett.*, 2008, **8**, 2150.
30 J. Li, X. Zhong, F. Cheng, J. R. Zhang, L. P. Jiang, and J. J. Zhu, *Anal. Chem.*, 2012, **84**, 4140.
31 Y. A. Shieh, S. J. Yang, M. F. Wei, and M. J. Shieh, *ACS Nano*, 2010, **4**, 1433.
32 F. Chen, Z. P. Cheng, J. Zhu, W. Zhang, and X. L. Zhu, *Eur. Polym. J.*, 2008, **44**, 1789.



 

33 L. Wang, W. J. Zhao, M. B. O'Donoghue, and W. H. Tan, *Bioconjugate Chem.* 2007, **18**, 297.
34 Z. S. Ge, Y. M. Zhou, J. Xu, H. W. Liu, D. Y. Chen, and S. Y. Liu, *J. Am. Chem. Soc.*, 2009, **131**, 1628.
35 B. Parrish, R. B. Breitenkamp, and T. Emrick, *J. Am. Chem. Soc.*, 2005, **127**, 7404.
36 F. Mahtab, J. W. Y. Lam, Y. Yu, J. Z. Liu, W. Z. Yuan, P. Lu, and B. Z. Tang, *Small*, 2011, 7, 1448.
37 K. Hayashi, M. Nakamura, H. Miki, S. Ozaki, M. Abe, T. Matsumoto, and K. Ishimura, *Adv. Funct. Mater.*, 2012, **22**, 3539.
38 Z. Zhou and C. J. Fahrni, *J. Am. Chem. Soc.*, 2004, **126**, 8862.
39 H. Ow, D. R. Larson, M. Srivastava, B. A. Baird, W. W. Webb, and U. Wiesner, *Nano Lett.*, 2005, **5**, 113.
40 D. Fischer, T. Bieber, Y. X. Li, H. P. Elsasser, and T. Kissel, *Pharm. Res.*, 1999, **16**, 1273.
41 H. Li, S. H. Park, J. H. Reif, T. H. LaBean, and H. Yan, *J. Am. Chem. Soc.*, 2004, **126**, 418.
42 E. A. Jares-Erijman, and T. M. Jovin, *Nat. Biotechnol.*, 2003, **21**, 1387.
43 S. H. Kim, J. H. Jeong, S. H. Lee, S. W. Kim, T. G. Park, *J. Controlled Release*, 2006, **116**, 123.

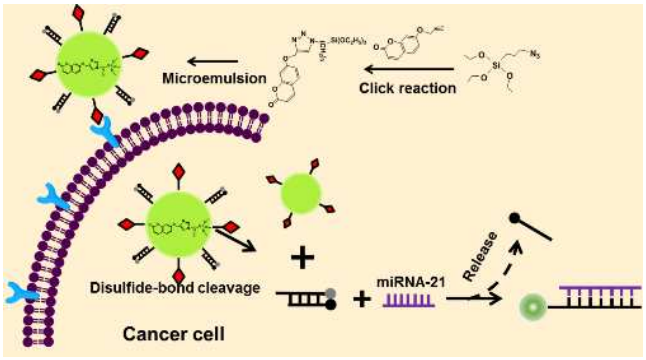


Fluorescent dye-doped silica nanoparticles prepared by silane derivatized coumarin for target-cell-specific delivery and intracellular microRNA imaging.